

Hypoxia Inhibits Cavin-1 and Cavin-2 Expression and Down-Regulates Caveolae in Adipocytes

Claire Regazzetti,* Karine Dumas,* Sandra Lacas-Gervais, Faustine Pastor, Pascal Peraldi, Stéphanie Bonnafous, Isabelle Dugail, Soazig Le Lay, Philippe Valet, Yannick Le Marchand-Brustel, Albert Tran, Philippe Gual, Jean-François Tanti, Mireille Cormont, and Sophie Giorgetti-Peraldi

INSERM Unité 1065 (C.R., K.D., F.P., Y.L.M.-B., J.-F.T., M.C., S.G.-P.), C3M, Mediterranean Research Centre for Molecular Medicine, Team 7 (Cellular and Molecular Physiopathology of Obesity and Diabetes), Unité de Formation et de Recherche (UFR) Médecine (C.R., K.D., F.P., P.P., S.B., Y.L.M.-B., A.T., P.G., J.-F.T., M.C., S.G.-P.), and INSERM Unité 1065 (S.B., A.T., P.G.), C3M, Mediterranean Research Centre for Molecular Medicine, Team 8 (Hepatic Complications in Obesity), University of Nice, Sophia Antipolis F-06204 Nice, France; Centre Commun de Microscopie Appliquée (S.L.-G.), University of Nice, Sophia Antipolis, UFR Sciences, Parc Valrose, F-06108 Nice, France; Unité Mixte de Recherche Centre National de la Recherche Scientifique 7277 (P.P.), Unité Mixte de Recherche INSERM Unité 1091, UFR Médecine, F-06107 Nice, France; Centre Hospitalier Universitaire de Nice, Digestive Center (S.B., A.T.), Nice F-06202, Cedex 3, France; INSERM Unité Mixte de Recherche S872 (I.D.), Centre de Recherche des Cordeliers, Eq8, F-75006 Paris, France; INSERM Unité 1063 (S.L.L.), Stress Oxydant et Pathologies Métaboliques, Institut de Biologie en Santé, F-49933 Angers, France; and INSERM Unité Mixte de Recherche 1048 (P.V.), Institut des Maladies Métaboliques et Cardiovasculaires, Université Paul Sabatier, F-31432 Toulouse, France

During obesity, a hypoxic state develops within the adipose tissue, resulting in insulin resistance. To understand the underlying mechanism, we analyzed the involvement of caveolae because they play a crucial role in the activation of insulin receptors. In the present study, we demonstrate that in 3T3-L1 adipocytes, hypoxia induces the disappearance of caveolae and inhibits the expression of Cavin-1 and Cavin-2, two proteins necessary for the formation of caveolae. In mice, hypoxia induced by the ligation of the spermatic artery results in the decrease of cavin-1 and cavin-2 expression in the epididymal adipose tissue. Down-regulation of the expression of cavins in response to hypoxia is dependent on hypoxia-inducible factor-1. Indeed, the inhibition of hypoxia-inducible factor-1 restores the expression of cavins and caveolae formation. Expression of cavins regulates insulin signaling because the silencing of cavin-1 and cavin-2 impairs insulin signaling pathway. In human, cavin-1 and cavin-2 are decreased in the sc adipose tissue of obese diabetic patients compared with lean subjects. Moreover, the expression of cavin-2 correlates negatively with the homeostatic model assessment index of insulin resistance and glycated hemoglobin level. In conclusion, we propose a new mechanism in which hypoxia inhibits cavin-1 and cavin-2 expression, resulting in the disappearance of caveolae. This leads to the inhibition of insulin signaling and the establishment of insulin resistance. (*Endocrinology* 156: 789–801, 2015)

Oxygen homeostasis is required for normal cell and tissue function. During hypoxia, cells establish cellular and metabolic responses to limit their oxygen consumption. Hypoxia decreases cell proliferation, switches metabolism

from oxidative phosphorylation to glycolysis, switches from oxidative glucose metabolism to reductive glutamine metabolism to promote fatty acid synthesis, and promotes angiogenesis to increase oxygen supply to cells (1–6).

ISSN Print 0013-7227 ISSN Online 1945-7170

Printed in U.S.A.

Copyright © 2015 by the Endocrine Society

Received August 5, 2014. Accepted December 8, 2014.

First Published Online December 18, 2014

* C.R. and K.D. contributed equally to the work.

Abbreviations: Ct, cycle threshold; DRM, detergent-resistant membrane; EM, electron microscope; Glut, glucose transporter; HIF, hypoxia-inducible factor; IR, insulin receptor; REDD1, regulated in development and DNA damage responses; siRNA, small interfering RNA.

Hypoxia also plays an important role in the dysfunction of the adipose tissue during obesity and the development of insulin resistance. Indeed, the expansion of the adipose tissue during obesity is associated with the development of hypoxic areas in obese mice (*ob/ob* mice and dietary induced obesity) and in overweight/obese patients (7–12).

Adipose tissue hypoxia, mainly through the activation of its master transcription factor, hypoxia-inducible factor (HIF)-1, induces a dysregulation of adipokines secretion, (7, 9, 13, 14), and contributes to the development of inflammation, by promoting macrophages and T lymphocytes accumulation and by inducing inflammatory phenotype in macrophages (9–11, 13, 15, 16). Modulation of HIF-1 α expression has an impact on the development of obesity and insulin resistance. Overexpression of HIF-1 α in adipocytes leads to the development of adipose tissue inflammation associated with fibrosis and insulin resistance in mice (17). Inhibition of HIF-1 α or HIF-1 β expression protects mice from obesity-induced glucose intolerance and insulin resistance and ameliorates adipose tissue dysfunction (18–22).

At the cellular level, hypoxia inhibits insulin-induced signaling pathways and induces insulin resistance in adipocytes through an HIF-1-dependent mechanism (23, 24). However, the precise molecular mechanisms by which hypoxia induces insulin resistance remains to be identified.

The insulin receptor is mainly localized within caveolae at the plasma membrane (25–27). Caveolae are small invaginations of the plasma membrane localized in lipid raft area and are particularly abundant in adipocytes in which they can represent up to 50% of the plasma membrane surface (28–30). Caveolae are involved in protein endocytosis, intracellular trafficking, lipid homeostasis, and signal transduction (30). Caveolae formation depends on the presence of specific proteins, such as the structural proteins caveolins and peripheral proteins cavins (28, 31). Caveolins 1–3 are essential for the formation of caveolae, and the absence of caveolin-1 expression leads to the disappearance of caveolae structures (32, 33). However, caveolins are not the sole proteins implicated in caveolae formation, and multiple proteins ensure the formation of caveolae. Among these proteins, cavins (PTRF/cavin-1, SDPR/cavin-2, SRBC/cavin-3 and MURC/cavin-4) are crucial for caveolae processing. Cavin complex is recruited to caveolin at the plasma membrane through membrane lipids and proteins interactions. Cavin-1 is required for caveolae formation, whereas cavin-2 is involved in the generation of caveolar membrane curvature (31, 34–37). Cavin-3 regulates caveolae endocytosis, whereas the expression of cavin-4 is restricted to the muscle (29, 38). The expression levels and cellular localizations of each protein

are tightly regulated and are required for the correct formation of caveolae. The absence of caveolin-1 or cavins leads to the loss of caveolae (39, 40). This absence of caveolae results in a variety of disease such as lipodystrophy, muscular dystrophy, cardiovascular disease, and cancer (41–43).

Some studies have shown that insulin receptor is localized within caveolae (26, 44, 45). A functional role of caveolae in insulin signaling is suggested by the observation that some lipodystrophic patients with severe insulin resistance present mutations in caveolin-1 or Cavin-1 (41, 42) and that the caveolar localization of the insulin receptor is necessary for its activation in adipocytes because caveolin-1-deficient cells have impaired insulin signaling (46).

To identify mechanisms implicated in the development of insulin resistance in response to hypoxia, we have investigated the effect of hypoxia on caveolae formation. We show that *in vivo* and in intact cells, hypoxia decreases cavin-1 and cavin-2 expression in adipocytes, associated with a loss of caveolae. Cavin expression is also decreased in adipose tissue from obese diabetic patients and its down-regulation in mouse adipocytes inhibits insulin signaling. Together, these observations suggest that hypoxia participates in the establishment of insulin resistance in adipose tissue through a down-regulation of caveolae that leads to a decrease in insulin signaling pathway.

Materials and Methods

Materials

Insulin was obtained from Life Technologies. Antibodies were obtained from the following companies: regulated in development and DNA damage responses (REDD1) and cavin-2 from Proteintech; phosphotyrosine from Cell Signaling Technology; insulin receptor (IR) and ERK2 from Santa Cruz Biotechnology; tubulin from Sigma-Aldrich; cavin-1 and flotillin from BD Biosciences; and glucose transporter (Glut)-1 from Abcam. Control small interfering RNA (siRNA) and siRNA directed against cavin-1, cavin-2, or HIF-1 α were purchased from Thermo Scientific. The primer sets for real-time PCR were purchased from Eurogentec. Culture media were obtained from Life Technologies. Inhibitors were obtained from Calbiochem.

Cell culture

3T3-L1 fibroblasts were obtained from the American Type Culture Collection (CL-173) and grown and induced to differentiate in adipocytes as previously described (23). Briefly, 3 days after confluence, 3T3-L1 fibroblasts were treated for 2 days with DMEM and 10% fetal calf serum (vol/vol) supplemented with isobutyl methylxanthine (250 nmol/L), dexamethasone (250 nmol/L), rosiglitazone (10 μ mol/L), and insulin (800 nmol/L) and then for two additional days with DMEM and 10% fetal calf serum containing 800 nmol/L insulin. The adipocytes were used between days 2 and 7 after the end of the differentiation protocol when the adipocyte phenotype appeared in more than 90% of the cells.

The isolation and properties of hMADS cells have been described by Plaisant et al (47). Adipocyte differentiation was performed as described previously (48). Confluent cells were cultured in DMEM/Ham's F12 media supplemented with transferrin (10 $\mu\text{g}/\text{mL}$), insulin (0.86 μM), T_3 (0.2 nmol/L), dexamethasone (1 $\mu\text{mol}/\text{L}$), isobutyl-methylxanthine (100 $\mu\text{mol}/\text{L}$), and rosiglitazone (500 nmol/L). Three days later, the medium was changed (dexamethasone and isobutylmethylxanthine were omitted).

Hypoxia treatment

For hypoxic treatment, the medium was replaced by DMEM containing 0.5% BSA and incubated within hypoxystation H35 (AES Chemunex) calibrated at 1% O_2 , 94% nitrogen, and 5% CO_2 for 16 hours.

Cell fractionation

Plasma membranes were prepared as previously described (49). OptiPrep fractionation (Sigma-Aldrich) was realized as fol-

lows: 3T3-L1 adipocytes were lysed with lysis buffer [50 mmol/L HEPES (pH 7.4), 150 mmol/L NaCl, 10 mmol/L EDTA, 10 mmol/L $\text{Na}_4\text{P}_2\text{O}_7$, 100 mmol/L NaF, 2 mmol/L vanadate, protease inhibitor cocktail (Complete; Roche)] containing Triton X-100 (1 μL per 10 mg protein) for 1 hour at 4°C. After shaking, the lysate was centrifuged 10 minutes at $110 \times g$. Six hundred microliters of supernatant mixed with 400 μL of OptiPrep density gradient medium (Sigma-Aldrich) were placed at the bottom of an ultracentrifuge tube and overlaid with 2 mL of 30% sucrose and 1 mL of lysis buffer. The gradient was formed after 2 hours of ultracentrifugation at 33 000 rpm in a TLS50 rotor. The mixture was divided into 10 fractions collected from the top of the tube and analyzed by Western blot.

Transfection of siRNA

3T3-L1 adipocytes were used for reverse transfection 7 days after the induction of differentiation. 3T3-L1 adipocytes were trypsinized, and control siRNA, or siRNA directed against HIF-1 α , cavin-1, or cavin-2 (40 pmol) were transfected using INTERFERin (Polyplus Transfection) according to the protocol of Kilroy et al (50). Briefly, siRNA complexes (80 nmol/L final concentration) were incubated with INTERFERin and lay onto the wells. 3T3-L1 adipocytes were trypsinized and added to the siRNA/INTERFERin complex solution. The adipocyte phenotype after transfection was assessed by visualization of lipid droplets, staining with oil red O, and expression of peroxisomal proliferator-activated receptor- γ protein (Regazzetti, C., K. Dumas, unpublished data).

Western blot analysis

Serum-starved cells were treated with ligands, chilled to 4°C, and washed with ice-cold PBS (6 mmol/L Na_2HPO_4 ; 1 mmol/L KH_2PO_4 , pH 7.4; 140 mmol/L NaCl; 3 mmol/L KCl) and solubilized with RIPA buffer [50 mmol/L Tris, pH 7.5; 150 mmol/L NaCl; 1% Nonidet P40; 0.1% sodium dodecyl sulfate; 0.5% Na deoxycholate; 1 mmol/L orthovanadate; 5 mmol/L NaF; 2.5 mmol/L $\text{Na}_4\text{P}_2\text{O}_7$; and Complete protease inhibitor cocktail (Roche Diagnostics)] for 30 minutes at 4°C.

Epididymal fat pads were frozen in liquid nitrogen and stored at -80°C until they were used. Tissues were solubilized by sonification in ice-cold buffer containing 20 mmol/L Tris (pH 7.5), 150 mmol/L NaCl, 2 mmol/L orthovanadate, 100 mmol/L NaF, 10 mmol/L $\text{Na}_4\text{P}_2\text{O}_7$, and completed with 1% Triton X-100 and Complete protease inhibitor cocktail (Roche Diagnostics).

Lysates were centrifuged (14 000 rpm) for 10 minutes at 4°C, and the protein concentration was determined using BCA protein assay reagent (Thermo

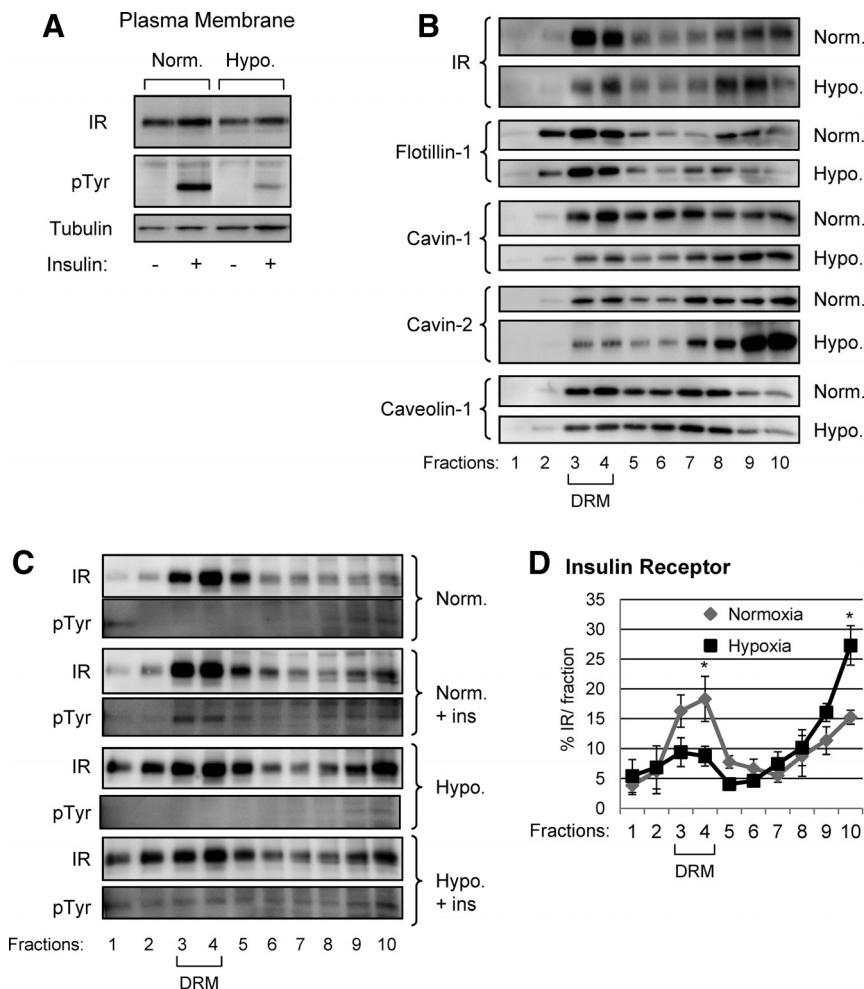


Figure 1. Hypoxia-induced delocalization of IR and caveolar proteins. A, 3T3-L1 adipocytes were incubated for 16 hours in normoxia or in hypoxia (1% O_2) before being stimulated with insulin (100 nM) for 5 minutes. Plasma membranes were analyzed by immunoblots with indicated antibodies. B, 3T3-L1 adipocytes were incubated for 16 hours in normoxia or in hypoxia (1% O_2). C, 3T3-L1 adipocytes were incubated for 16 hours in normoxia or in hypoxia (1% O_2) before being stimulated with insulin (100 nM) for 5 minutes. Cell lysates were separated into 10 fractions from the lightest (fraction 1) to the heaviest (fraction 10) using OptiPrep density gradient fractionation (Sigma-Aldrich) and analyzed by Western blots with indicated antibodies. D, Quantification of IR of three experiments is shown. *, $P < .05$. Hypo, hypoxia; Norm, normoxia.

Fisher Scientific). Cell lysates were analyzed by Western blot. Immunoblots were revealed using a Fujifilm LAS-3000 imaging system. Quantifications were realized using Fujifilm MultiGauge or ImageJ softwares (National Institutes of Health, Bethesda, Maryland).

Hypoxia of epididymal adipose tissue by ligation of spermatic artery

C57BL6/J mice were exposed to a 12-hour light, 12-hour dark schedule and had free access to water and standard chow diet. Mice were anesthetized, and the left spermatic artery was ligatured to induce hypoxia on the fat pad for indicated periods of time. The right spermatic artery was not ligatured, and the fat pad was used as an internal control. Mice woke up from the surgery and were kept for indicated periods of time before being killed by cervical dislocation. Epididymal adipose tissues were removed, freeze clamped in liquid nitrogen, and stored at -80°C until used. The Principles of Laboratory Animal Care (National Institutes of Health publication number 85–23, revised 1985 (<http://grants1.nih.gov/grants/olaw/references/phspol.htm>) as well the European Union guidelines on animal laboratory care (<http://ec.europa.eu/>

environment/chemicals/lab_animals/legislation_en.htm) were followed. All procedures were approved by the Animal Care Committee of the Faculty of Medicine of the Nice-Sophia Antipolis University (Nice, France).

Obese patients

Morbidly obese patients ($n = 8$ obese and $n = 7$ obese diabetic) were recruited through the Department of Digestive Surgery and Liver Transplantation (Nice hospital) where they underwent bariatric surgery for their morbid obesity. Bariatric surgery was indicated for these patients in accordance with French guidelines. Exclusion criteria were the presence of a hepatitis B or hepatitis C infection, excessive alcohol consumption (>20 g/d) or another cause of chronic liver disease as previously described (51–53). The characteristics of the study groups are described in Supplemental Table 1. Before surgery, fasting blood samples were obtained and used to measure alanine amino transferase, aspartate aminotransaminase, glucose, and insulin. Insulin resistance was calculated using the homeostatic model assessment index for insulin resistance (HOMA-IR) (54). Abdominal sc adipose tissue was obtained during surgery. Control

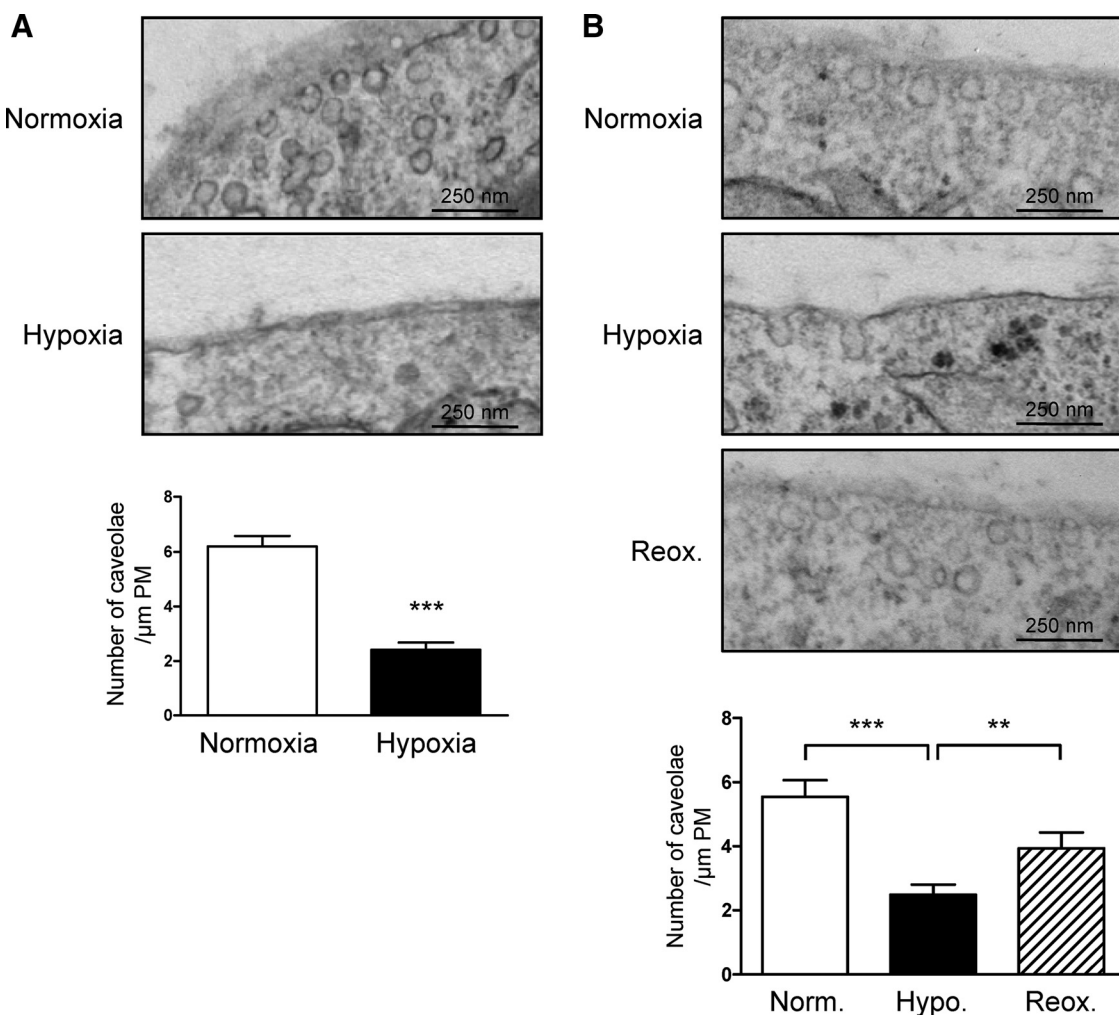


Figure 2. Hypoxia induced the loss of caveolae in 3T3-L1 adipocytes. 3T3-L1 adipocytes were incubated for 16 hours in normoxia or in hypoxia (1% O_2) (A) or reoxygenated (B) for 1 hour. Caveolae structure were identified by transmission EM. Quantification is performed after counting the number of caveolae and are expressed as number of caveolae per micrometer of plasma membrane (PM). ***, $P < .0001$; **, $P < .01$. Number of caveolae counted is as follows: normoxia: 1938, hypoxia: 1597 (A); normoxia: 1105, hypoxia: 1125, reox: 731 (B). Reox, reoxygenated.

sc adipose tissue was obtained from four lean subjects (two females and two males; aged 37.3 ± 11.5 y; body mass index of 20.9 ± 0.5 kg/m²) undergoing lipectomy for cosmetic purposes. Informed written consent was obtained from all subjects for this study, which was set up in accordance with French legislation regarding ethics and human research (Huriet-Serusclet). The Comité Consultatif de Protection des Personnes dans la Recherche Biomédicale de Nice approved the study (protocol 07/04:2003, number 03.017).

Real-time quantitative PCR analysis

Cells and murine tissues

RNA was isolated from adipocytes or epididymal fat pads (TRIZOL; Invitrogen), and cDNA was synthesized using Tran-

scriptor first-strand cDNA synthesis kit (Roche Diagnostics). Real-time quantitative PCR was performed with sequence detection systems (StepOne; Applied Biosystems) and SYBR Green dye. Gene expression values were calculated based on the comparative cycle threshold (Ct) method ($2^{-\Delta\Delta Ct}$). The levels of mRNA were normalized to the expression value of the housekeeping gene 36B4 and expressed relative to the mean of the group of normoxic controls. The primer sequence can be obtained upon request.

Human tissues

Total RNA was extracted from human tissues using RNeasy minikit (QIAGEN) and treated with Turbo DNA-free (Applied Biosystems) following the manufacturer's protocol. The quantity and quality of the RNA were determined using the Agilent 2100 Bioanalyzer with an RNA 6000 Nano kit (Agilent Technologies). Total RNA (1 μ g) was reverse transcribed with a high-capacity cDNA reverse transcription kit (Applied Biosystems). Real-time quantitative PCR was performed in duplicate for each sample using the StepOne real-time PCR system (Applied Biosystems). The TaqMan gene expression assays were purchased from Applied Biosystems: *Cavin-2* (serum deprivation response, cavin-2) (Hs00190538_m1); *Cavin-1* (polymerase I and transcript release factor, cavin-1) (Hs00396859_m1); *Glut4* (*SLC2A4*) (Hs00168966_m1); *HIF-1A* (hypoxia inducible factor-1) (Hs00153153_m1); and *RPLP0* (ribosomal phosphoprotein large P0) (Hs99999902_m1). Gene expression values were normalized to the expression value of the housekeeping gene *RPLP0* and calculated based on the comparative Ct method ($2^{-\Delta\Delta Ct}$) as described by the manufacturer's protocols.

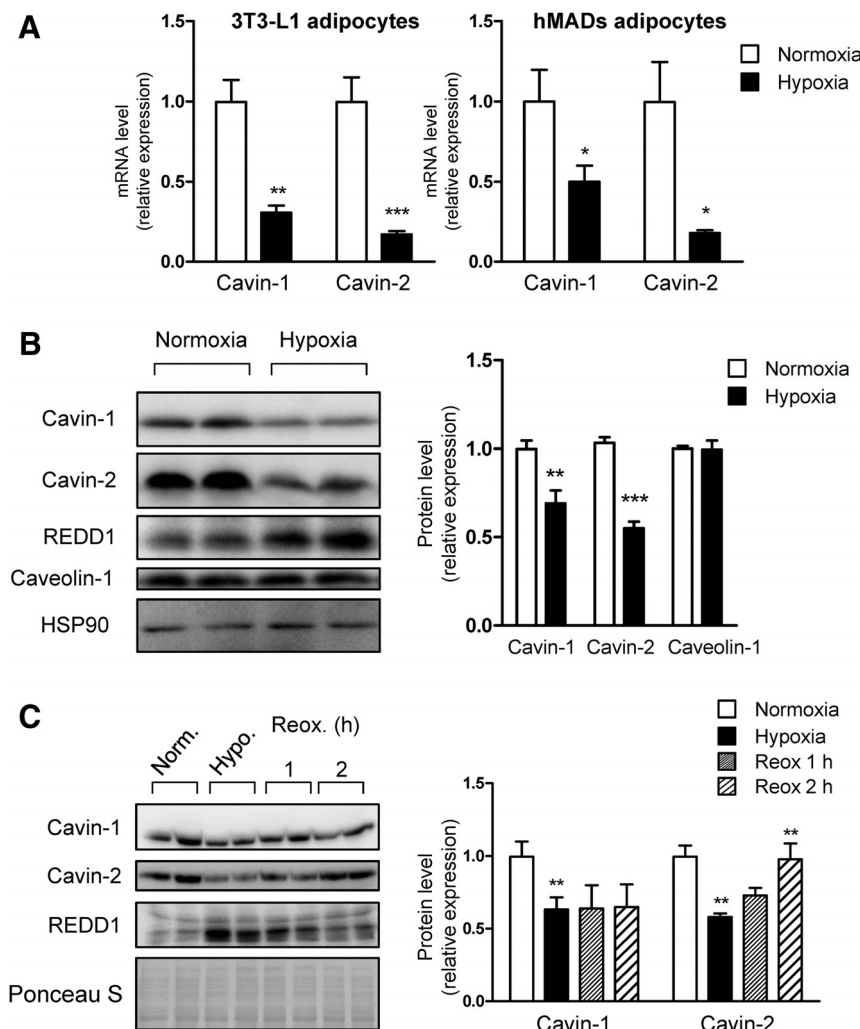


Figure 3. Hypoxia decreased cavin-1 and cavin-2 expression. A, 3T3-L1 adipocytes and hMADS adipocytes were incubated for 16 hours in normoxia or in hypoxia (1% O₂), and mRNA expression was determined by quantitative RT-PCR. B, 3T3-L1 adipocytes were incubated for 16 hours in normoxia or in hypoxia (1% O₂) and protein expression was analyzed by specific immunoblots. Quantification of relative expression of cavin-1, cavin-2, and caveolin-1 (normalized to tubulin protein level) is shown (n = 8). C, 3T3-L1 adipocytes were incubated for 16 hours in normoxia or in hypoxia (1% O₂), or reoxygenated for 1 or 2 hours, and protein expression was analyzed by specific immunoblots. Quantification of relative expression of cavin-1 and cavin-2 is shown (n = 3). Ponceau S is used as a loading control. ***, P < .0001; **, P < .01; *, P < .05. HSP, heat shock protein; Hypo, hypoxia; Norm, normoxia.

Electron microscopy

For ultrastructural analysis, cells were fixed in 1.6% glutaraldehyde in 0.1 M phosphate buffer (pH 7.4) at 4°C, rinsed in 0.1 mol/L cacodylate buffer, and postfixed for 1 hour in 1% osmium tetroxide and 1% potassium ferrocyanide in 0.1 mol/L cacodylate buffer to enhance the staining of membranes. Cells were rinsed in cold distilled water, quickly dehydrated in cold ethanol, and lastly embedded in epoxy resin. Contrasted ultrathin sections (70 nm) were analyzed under a JEOL 1400 transmission electron microscope (EM) mounted with a Morada Olympus charge-coupled device camera.

Statistical analysis

The statistical significance of the differential gene expression between two

groups was determined using the nonparametric Mann-Whitney test with the δ Ct of each group. Correlations were analyzed using the Spearman's rank correlation test. $P < .05$ is considered as significant.

Results

Hypoxia-modulated insulin receptor localization in 3T3-L1 adipocytes

Hypoxia inhibited insulin-tyrosine phosphorylation of insulin receptor in adipocytes (23). Because the localization of

insulin receptor in caveolae microdomains in plasma membrane is required for its activation, we first evaluated its cellular localization and phosphorylation in normoxia and in response to hypoxia. 3T3-L1 adipocytes were stimulated with insulin, plasma membranes were extracted, and insulin receptor within this fraction was analyzed by Western blots. Hypoxia inhibited insulin receptor tyrosine phosphorylation without significantly modifying its amount at the plasma membrane (Figure 1A). The distribution of the IR was then evaluated by cellular fractionation [using the Opti-Prep density gradient method (Sigma-Aldrich)] in normoxia or in

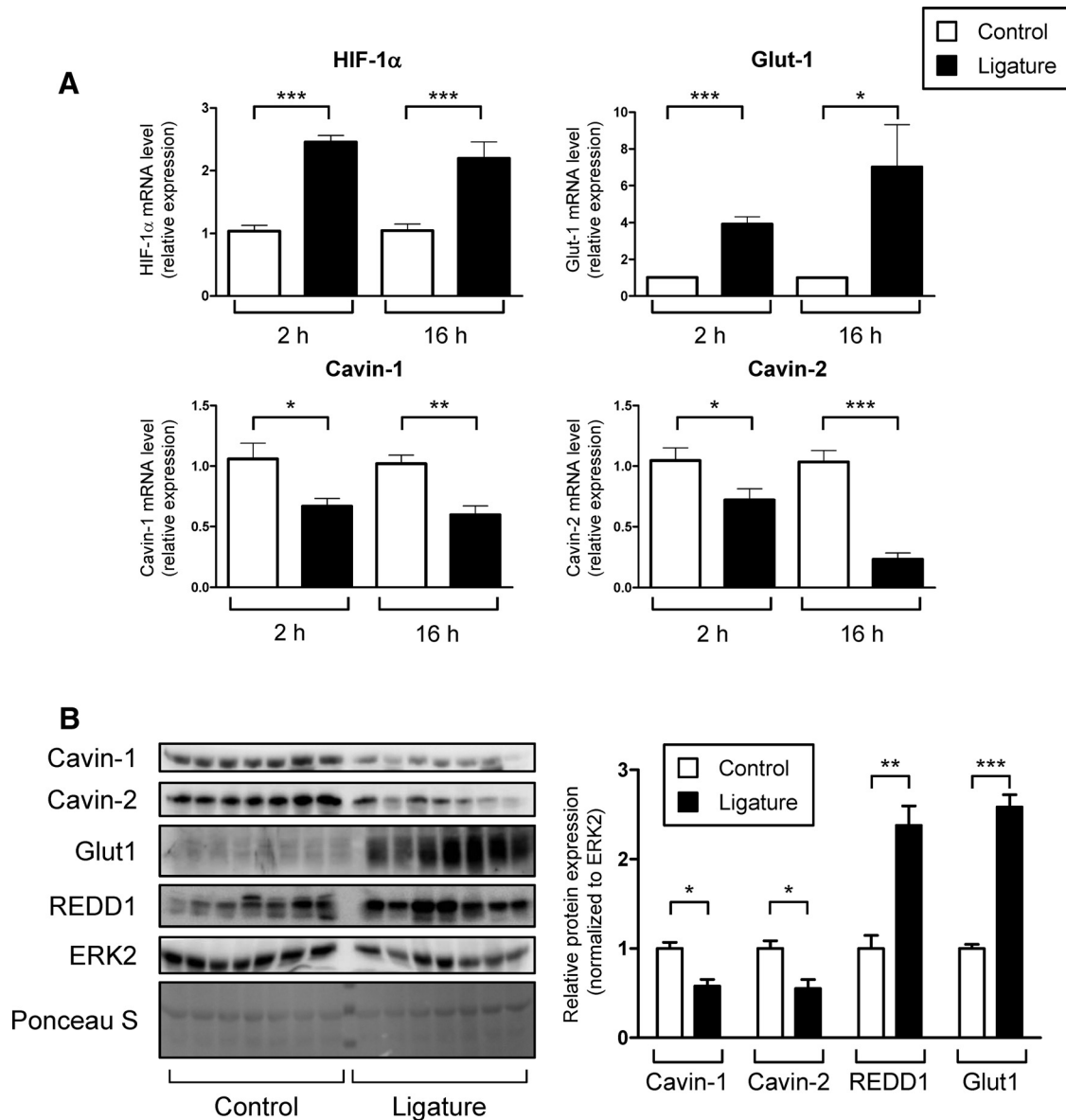


Figure 4. Ligature of spermatic artery induced hypoxia of epididymal adipose tissue and decreased cavin-1 and cavin-2 expression. Spermatic artery of mice were ligatured as described in *Materials and Methods*. Epididymal adipose tissues were removed and used to analyze mRNA expression after 2 and 16 hours (A) or protein expression after 16 hours (B). A, Results are expressed in a relative expression, with the control value taken as 1 and are the means \pm SE of eight mice in each group. B, Quantification of the relative expression of cavin-1, cavin-2, Glut-1, and REDD1 (normalized to ERK2) is shown (each point represents one mouse, $n = 7$). Ponceau S is shown as loading control. *, $P < .05$; **, $P < .01$; ***, $P < .001$.

hypoxia. Cell lysates were resolved into 10 fractions from the lightest (fraction 1) to the heaviest (fraction 10) and analyzed by Western blots (Figure 1B). Detergent-resistant membrane (DRM) fractions were identified by immunoblotting of flotillin-1. Flotillins were initially discovered as caveolae-associated integral proteins (55), but they still localize to lipid-raft membranes in the absence of caveolins (56, 57). Therefore, although they are not exclusively located in caveolar domains, flotillins are considered as a good marker for total lipid rafts, biochemically preserved, and recovered in DRMs. In normoxia, IR was mainly located within the DRM fractions (3 and 4) to heavier fractions (Figure 1B). In Figure 1C, 3T3-L1 adipocytes were stimulated with insulin prior to cellular fractionation. In normoxia, insulin stimulated the tyrosine phosphorylation of its receptor located in DRM fractions. In hypoxia, the IR in fractions 3 and 4 was no longer phosphorylated in response to insulin.

Hypoxia induced the disappearance of caveolae in 3T3-L1 adipocytes

Because hypoxia inhibited IR phosphorylation and distribution at the plasma membrane, we evaluated the effect of

hypoxia on the integrity of caveolae. We evaluated the distribution of cavin proteins, cavin-1 and cavin-2, in response to hypoxia by cell fractionation (Figure 1B). In normoxia, cavin-1 and cavin-2 were mainly detected in fractions 3 and 4 and in fewer amount in heavier fractions. Hypoxia induced a change in the distribution of these proteins. Indeed, cavin-1 and cavin-2 amounts shifted from lightest fractions to heavier fractions (fractions 9 and 10). This modification of protein distribution suggests that hypoxia could affect the formation of caveolae in adipocytes.

The integrity of caveolae in 3T3-L1 adipocytes incubated in normoxia or hypoxia was determined by transmission EM. In Figure 2A, caveolae were detected near the plasma membrane in 3T3-L1 adipocytes. Hypoxia incubation induced the disappearance of caveolae in this region. We have previously demonstrated that the inhibition of the insulin signaling pathway by hypoxia can be reversed after cell reoxygenation (23). Accordingly, the reoxygenation of adipocytes restored the presence of caveolae at the cell surface (Figure 2B).

Hypoxia decreased expression of cavin-1 and cavin-2

Cell fractionation is not a reflection of the quantity of proteins within the cell, but it rather reflects their cellular localization. Because a decrease in cavin and caveolin has been shown to alter caveolae structure (39, 40, 58), we investigated whether the expression of these proteins was modified by hypoxia in murine (3T3-L1) and human (hMADS) adipocytes. In 3T3-L1 and hMADS adipocytes, hypoxia inhibited the expression of mRNA of cavin-1 and cavin-2 (Figure 3A). In 3T3-L1 adipocytes, hypoxia decreased significantly the protein expression of cavin-1 and cavin-2 (Figure 3B). In contrast, the expression of caveolin-1 was not modified after hypoxia treatment (Figure 3B). Because reoxygenation restored caveolae at the cell surface, we have determined the effect of reoxygenation on cavin-1 and cavin-2 expression in 3T3-L1 adipocytes. As shown in Figure 3C, reoxygenation restored cavin-2 expression without any significant effect on cavin-1 protein expression.

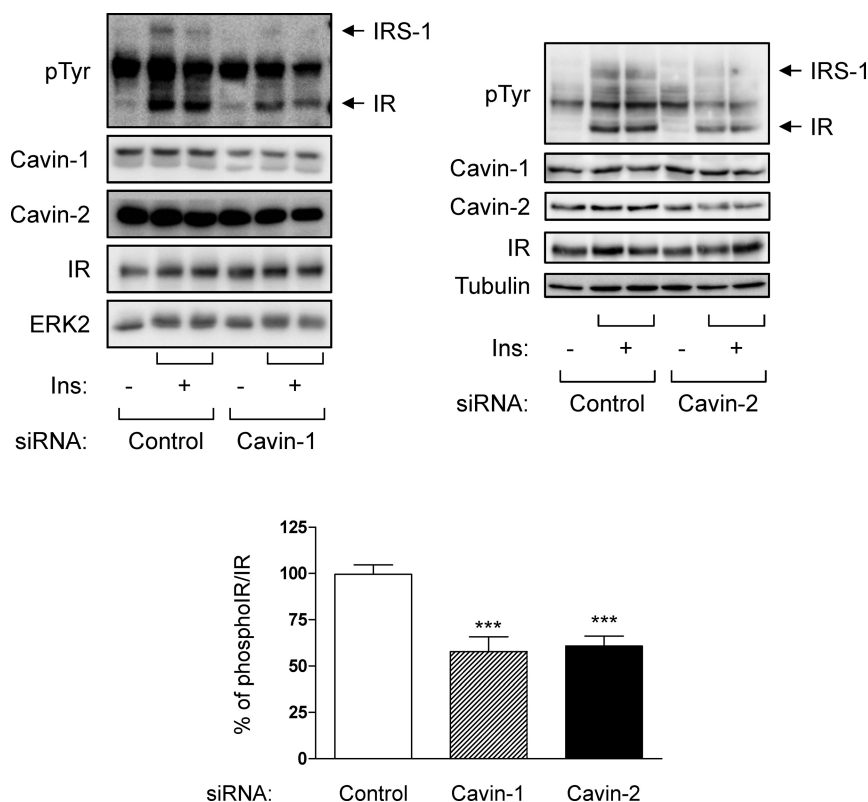


Figure 5. Inhibition of cavin-1 and cavin-2 expression inhibited insulin receptor phosphorylation. 3T3-L1 adipocytes were transfected with control or siRNA against cavin-1 or cavin-2. Forty-eight hours after transfection, 3T3-L1 adipocytes were stimulated with insulin (100 nM) for 5 minutes. Proteins were analyzed by immunoblots using indicated antibodies. Phosphorylation of insulin receptor is normalized using insulin receptor, and quantification of three independent experiments in duplicate is shown. ***, $P < .001$. Ins, insulin.

To study the effect of hypoxia on protein expression in mice, we have set up a protocol to induce hypoxia in epididymal adipose tissue by the ligation of spermatic artery. The left spermatic artery of C57BL6/J mice was ligatured to induce hypoxia on the fat pad for the indicated periods of time. The right spermatic artery was not ligatured, and the fat pad was used as an internal control. Ligation of spermatic artery induced hypoxia of the epididymal adipose tissue, detected by the increase of HIF-1 α and Glut-1 mRNA expression (Figure 4A). Hypoxia decreased cavin-1 and cavin-2 mRNA expression in epididymal fat pads as soon as after 2 hours of ligation. Protein expression was also studied, and we observed that hypoxia inhibited cavin-1 and cavin-2 expression in hypoxic fat pads (Figure 4B). As control, the expression of REDD1, a hypoxia-induced protein (59, 60), and Glut-1 was increased. ERK2 and Ponceau S are shown as loading control.

Decrease in expression of cavin-1 and cavin-2 inhibited insulin signaling pathway in adipocytes

Because cavins are key components of caveolae, we investigated the outcome of the decrease in expression of cavin-1 and cavin-2 on insulin receptor activity. 3T3-L1 adipocytes were transfected with siRNA against cavin-1 or cavin-2 and stimulated with insulin (Figure 5). Transfection of cavins siRNA decreases the expression of cavins to a level similar to hypoxia treatment. Down-regulation

of the expression of cavin-1 or cavin-2 inhibited IR tyrosine phosphorylation (respectively, 43% \pm 8% and 40% \pm 5% of inhibition).

Hypoxia decreased the expression of cavin-1 and cavin-2 through a HIF-1 α dependent mechanism

Because the expression of cavin-1 and cavin-2 is regulated by hypoxia, we investigated the implication of HIF-1 transcription factor in this mechanism. Indeed, we previously reported that HIF-1 is implicated in the inhibition of insulin signaling in response to hypoxia (23). 3T3-L1 adipocytes were transfected with siRNA against HIF-1 α or treated with echinomycin, a HIF-1 α inhibitor, prior to being exposed to hypoxia for 16 hours (Figure 6).

The decrease of expression of cavin-1 and cavin-2 induced by hypoxia was reversed after inhibition of HIF-1. Efficiency of echinomycin and silencing of HIF-1 α was evaluated by the down-regulation of REDD1 at the protein level (Figure 6) as previously reported (61). These results demonstrate that the expression of cavin-1 and cavin-2 was regulated by HIF-1 dependent mechanisms.

We then determined the involvement of HIF-1 in caveolae formation (Figure 7). Inhibition of HIF-1 α by siRNA restored the number of caveolae at the cell surface in hypoxia (Figure 7A). In parallel, the activation of HIF-1 by

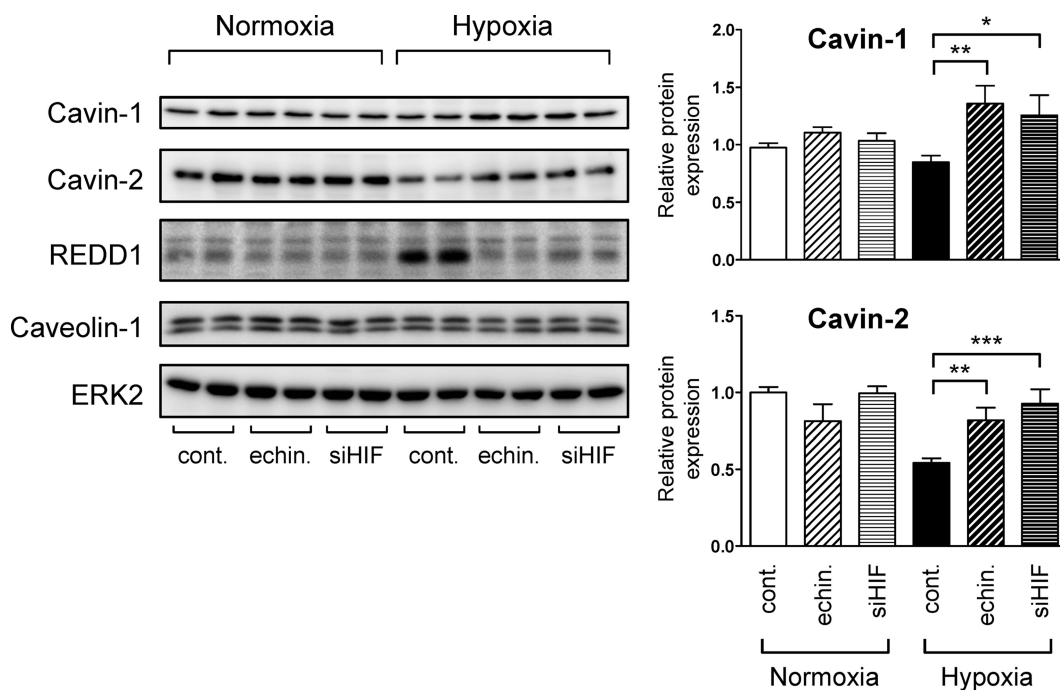


Figure 6. Inhibition of HIF-1 α restored cavin-1 and cavin-2 expression in hypoxia in 3T3-L1 adipocytes. 3T3-L1 adipocytes were transfected with control or HIF-1 α siRNA. Forty-eight hours after transfection, 3T3-L1 adipocytes were treated without or with echinomycin (20 nM) for 16 hours and incubated in normoxia or in hypoxia (1% O₂). Proteins were analyzed by immunoblots using the indicated antibodies. Quantification of expression of proteins is normalized using tubulin (n = 3 independent experiments in duplicate). *, P < .05; **, P < .01; ***, P < .001. cont, control.

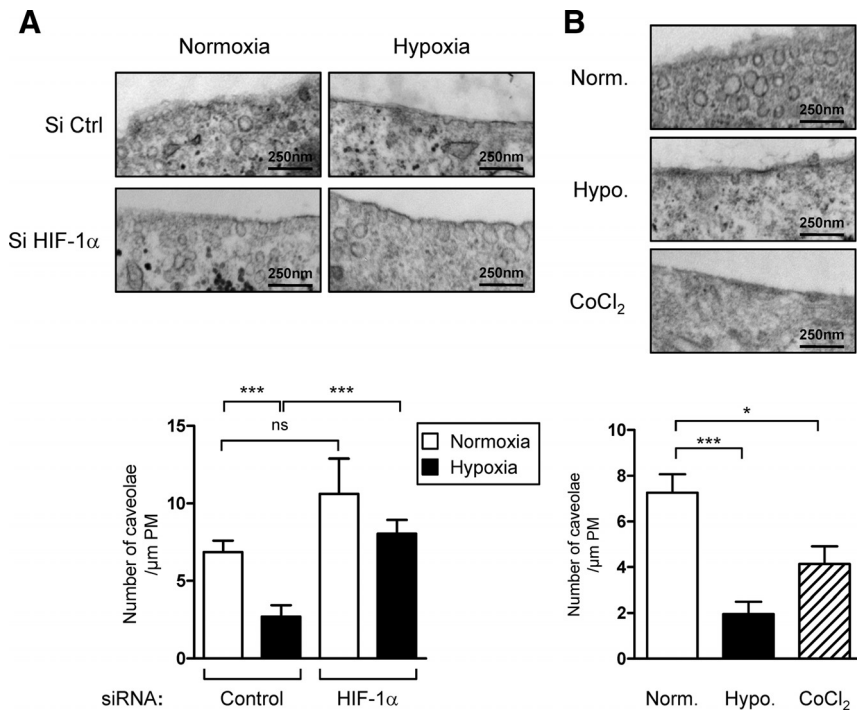


Figure 7. Hypoxia induced the loss of caveolae through HIF-1 activity in 3T3-L1 adipocytes. A, 3T3-L1 adipocytes were transfected with control or HIF-1 α siRNA before being incubated in normoxia or in hypoxia for 16 hours. B, 3T3-L1 adipocytes were incubated for 16 hours in normoxia or in hypoxia (1% O₂) or treated with CoCl₂ (200 μ M). Caveolae structures were identified by transmission EM. Quantification is performed after counting the number of caveolae and are expressed as the number of caveolae per micrometer of plasma membrane (PM). ***, $P < .0001$; *, $P < .05$. Numbers of caveolae counted are as follows: control siRNA normoxia, 431; hypoxia, 245; HIF-1 siRNA normoxia, 614; hypoxia, 728 (A); normoxia, 401; hypoxia, 226; CoCl₂, 1241 (B). Hypo, hypoxia; Norm, normoxia.

CoCl₂ inhibited the caveolae at the cell surface (Figure 7B). Taken together, these observations suggest that hypoxia decreased caveolae formation through a HIF-1-dependent pathway.

Insulin resistance is associated with a decreased in the expression of cavin-1 and 2 in adipose tissue of obese patients

Because obesity is associated with the hypoxia of the adipose tissue and insulin resistance, we evaluated the expression of HIF-1 α , cavin-1, and cavin-2 in sc adipose tissue of lean subjects and obese patients without or with type 2 diabetes. As shown in Figure 8A, HIF-1 α mRNA expression was increased in the adipose tissues of obese and obese diabetic patients. In contrast, cavin-1 and cavin-2 were decreased only in sc adipose tissue of obese diabetic patients compared with lean subjects (Figure 8A). Furthermore, cavin-2 correlated positively with cavin-1 level and negatively with HOMA-IR (index used to evaluate insulin resistance) and glycated hemoglobin level (evaluating the average plasma glucose concentration over prolonged periods of time), which reflect the risk of developing diabetes-related complications.

This indicates that the decreased expression of cavin in adipose tissue could be associated with insulin resistance.

Discussion

Hypoxia promotes inflammation, impairs adipose tissue endocrine function, and contributes to insulin resistance (7–10, 12, 13, 62). We and others (23, 24) have demonstrated that hypoxia induces insulin resistance in adipocytes through the inhibition of the insulin receptor autophosphorylation and signaling pathway. In the attempt to understand the mechanisms implicated, we demonstrate that hypoxia inhibits the expression of caveolar proteins cavin-1 and cavin-2 in adipocytes, which is accompanied by the loss of caveolae at the plasma membrane. Moreover, cavin-1 and cavin-2 expression is decreased in adipose tissue from obese diabetic patients. These observations prompt us to propose that hypoxia induces insulin resistance through the down-regulation of caveolae, leading to the impaired insulin signaling pathway.

Caveolae are abundant in adipocytes in which they play a major role in insulin signaling (27, 44). IRs are mainly localized at the plasma membrane in caveolae, with little insulin receptors found outside from the caveolae (26, 44, 45, 63). Caveolar localization of insulin receptor is required for its activation. Indeed, the modulation of caveolin-1 expression and caveolae structures affects insulin signaling pathway (27, 45, 63). Moreover, the absence of cavin-1 and cavin-2 in 3T3-L1 adipocytes inhibits insulin-induced activation of its receptor. This is in accordance with the observation that the deficiency of cavin-1 generates mice without caveolae and resistant to diet-induced obesity with an abnormal lipid metabolism and insulin signaling pathway (39). Hypoxia regulates only cavin expression but not the expression of caveolin-1. The expression and distribution of cavin might be affected, whereas the caveolin-1 distribution or expression seems unaltered but still leads to caveolae disassembly. Briand et al (64) have recently reported that during extreme fat cell shrinkage in adipocytes, caveolin-1 expression was unaffected, whereas cavin-1 and cavin-2 were targeted to degradation, resulting in caveolae disassembly. The deletion of cavin-2 in endothe-

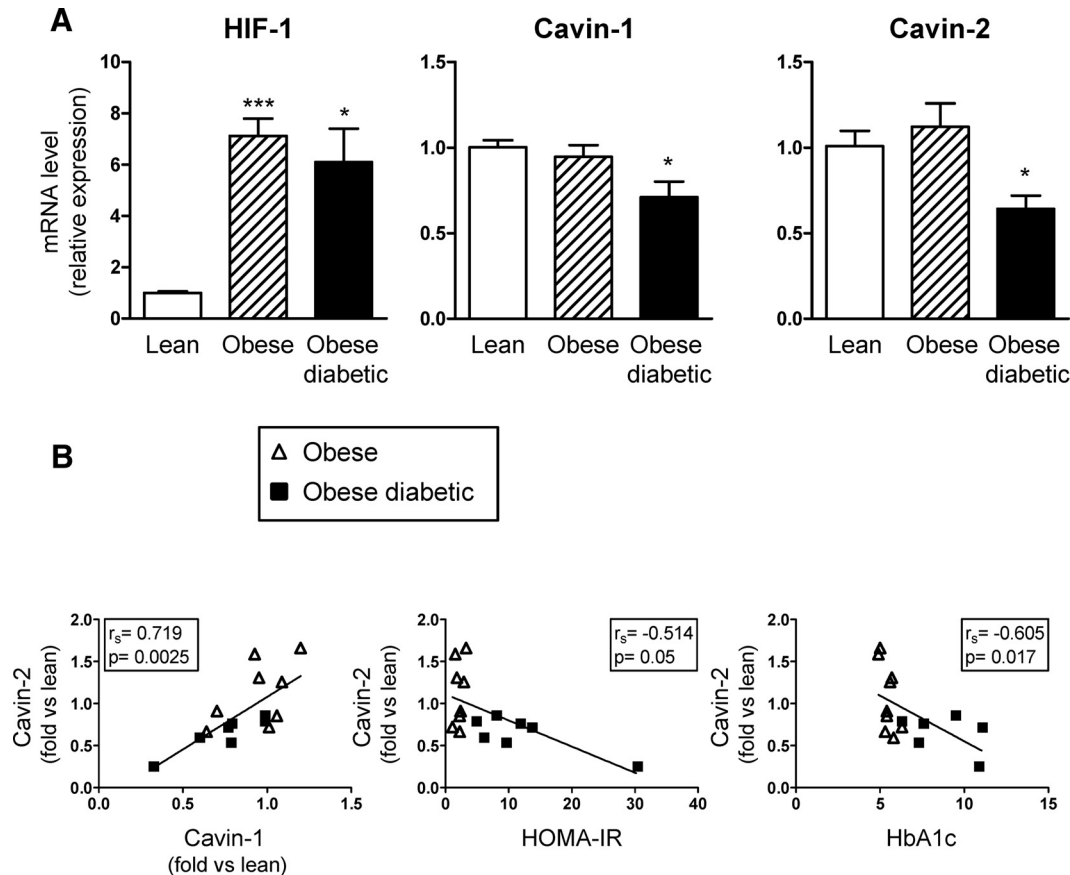


Figure 8. Cavin-1 and cavin-2 expression was decreased in adipose tissue of obese diabetic patients. A, Biopsies of sc adipose tissues from lean ($n = 4$), obese without ($n = 8$), or obese with diabetes ($n = 7$) were collected. Total RNAs were extracted and the relative amount of cavin-1, cavin-2, and HIF-1 α were determined by real-time quantitative PCR. Results are expressed in arbitrary units with the control value (lean subjects) taken as 1 and are the means \pm SE of the number of subjects in each group. *, $P < .05$; ***, $P < .0001$. B, Correlations between cavin-2 and cavin-1 expression levels, cavin-2 and HOMA-IR, and HbA1c were analyzed using a Spearman's rank correlation test (white triangle, obese patients; black square, obese diabetic patients). HbA1c, glycated hemoglobin.

lial cells causes flattening of caveolae perturbing neither caveolin-1 expression nor oligomerization (65). Therefore, cavins can be viewed as critical caveolar organizers whose distribution or expression would influence caveolae integrity. In this regard, cavins appear as early sensors of physiological events of caveolae dynamics. Moreover, our observations clearly demonstrate that insulin receptor localization within caveolae is mandatory for its activation.

During obesity, adipose tissue oxygen tension is decreased to reach 2% (8–11). Hypoxia regulates inflammation and angiogenesis but also general cellular metabolism including glucose use. In the present study, we demonstrate that hypoxia can regulate caveolae formation through the regulation of cavin proteins expression. Indeed, hypoxia decreases the expression of cavin-1 and cavin-2, in murine and human adipocytes, and also in a model of ligation of the spermatic artery to induce hypoxia of the epididymal adipose tissue. Moreover, this inhibition of the expression of cavins is accompanied by the loss of caveolae at the surface of 3T3-L1 adipocytes. Cavins con-

tribute to the stability of caveolae because the down-regulation of cavin-1 shortens the half-life of caveolin-1, likely targeting caveolin-1 for lysosomal degradation (36, 37). Cavin proteins might also serve as a bridge for other caveolar proteins such as EH domain containing 2 (66) and organize cytoskeleton connection (39). Cavin redistribution to cytosolic compartments might be linked to cavin degradation, an event reported in adipocytes and in others cells to signal caveolae disassembly (40, 64).

Hypoxia has been shown to regulate gene expression in human adipocytes. Among 1346 genes differently regulated by hypoxia, cavin-2 expression is decreased (3.76-fold change) compared with the normoxic conditions (67). Inhibition of cavin-1 and cavin-2 expression is dependent on the HIF-1 transcription factor. The molecular mechanisms implicated in the regulation of cavin-1 and cavin-2 expression remain unknown. A sequence analysis reveals that cavin-2 promoter contains HRE sequences, but we cannot rule out that other transcription factors could participate in the regulation of the expression of cavins. For instance, Krüppel-like factor-7, activating transcription

factor, Fos-like antigen 2, and Jun transcription factors are involved in the regulation of gene expression in response to hypoxia in adipocytes, and this activation requires HIF-1 α (68).

Insulin resistance and type 2 diabetes are linked to obesity. Hypoxia has been proposed to play a crucial role in the establishment of adipose tissue insulin resistance, and we found that HIF-1 α expression is increased in adipose tissue during obesity. This is in agreement with previous studies showing an up-regulation of the expression of HIF-1 α mRNA in adipose tissue during obesity in mice (genetic obesity or high fat diet) (10, 11, 24, 69) and in humans (70). Because the expression of HIF-1 α is not different between obese and obese diabetic patients, we cannot rule out that the activity of HIF-1 will be modified between obese and obese diabetic patients because HIF-1 α regulation mainly requires posttranslational mechanisms (3). The expression of cavin-1 and cavin-2 is significantly inhibited in adipose tissue of obese patients with type 2 diabetes. The decrease in cavin-2 expression correlated with insulin resistance as evaluated by HOMA-IR. Dysfunctional caveolae results in insulin resistance because patients with mutations of caveolin-1 or cavin-1 display lipodystrophy phenotype characterized by insulin resistance development (41, 42, 71, 72). Caveolae dysfunction is also implicated in several pathologies, such as muscular dystrophies, pulmonary hypertension in chronic obstructive pulmonary disease, bladder smooth muscle hypertrophy, and cancer (73, 74). Even if the role of caveolae in cancer development remains unclear, expression of cavin-1, cavin-2, and cavin-3 is down-regulated in breast cancer (75, 76). Because no correlation between HIF-1 α and cavin-2 has been revealed, this suggest that others factors, in addition to HIF-1, could participate the regulation of the expression of cavins during diabetes.

In conclusion, we propose that during obesity, hypoxia induces insulin resistance through the regulation of cavins expression. Inhibition of cavin-1 and cavin-2 expression induces the disappearance of caveolae leading to the inhibition of insulin signaling and establishment of insulin resistance.

Acknowledgments

We acknowledge Frédéric Bost (INSERM Unité 1065) for careful reading, Jerome Gilleron (INSERM Unité 1065) for helpful discussions, and Johanna Chiche (INSERM Unité 1065) for reagents. We gratefully acknowledge Veronique Corcelle and the C3M animal facility team for their valuable assistance with animal care. We also greatly acknowledge the Centre Commun de

Microscopie Appliquée (Université de Nice Sophia Antipolis, Microscopy and Imaging Platform, Côte d'Azur).

Address all correspondence and requests for reprints to: Sophie Giorgetti-Peraldi, PhD, INSERM Unité 1065, Centre Méditerranéen de Médecine Moléculaire, Bâtiment ARCHIMED, 151 Route Saint Antoine de Ginestière, BP 2 3094, F-06204 Nice Cedex 3, France. E-mail: peraldis@unice.fr.

Author contributions include the following: C.R. and K.D., designed and performed the experiments, researched and analyzed the data, contributed to the discussion, and reviewed the manuscript. S.L.-G., F.P., and S.B. contributed to the experiments and discussed the data. I.D., S.L.L., P.V., Y.L.M.-B., A.T., P.G., J.F.T., and M.C. analyzed the data, contributed to the discussion, and reviewed the manuscript. P.P. contributed to the experiments, discussed the data, and wrote and reviewed the manuscript. S.G.P. designed and performed the experiments, analyzed the data, and wrote and edited the manuscript. S.G.P. is the guarantor of this work, had full access to all the data, and takes full responsibility for the integrity of data and the accuracy of the data analysis.

This work was supported by INSERM (France), Société Francophone du Diabète, SFD/Roche Pharma, European Foundation for the study of Diabetes/Lilly European Diabetes Research Programme, Agence Nationale de la Recherche (Grant ANR-09-GENO-036 and "Investments for the Future" Labex Signalife Grant ANR-11-LABX-0028-01), the University of Nice-Sophia Antipolis, Region Provence-Alpes-Cote-d'Azur, Conseil Général des Alpes Maritimes, and the Programme Hospitalier de Recherche Clinique (Centre Hospitalier Universitaire of Nice). C.R. is a recipient of a fellowship of the Société Francophone du Diabète, and F.P. is a recipient of a fellowship from the Ministère de la Recherche et de l'Éducation.

Disclosure Summary: The authors have nothing to disclose.

References

1. Wise DR, Ward PS, Shay JE, et al. Hypoxia promotes isocitrate dehydrogenase-dependent carboxylation of α -ketoglutarate to citrate to support cell growth and viability. *Proc Natl Acad Sci USA*. 2011;108(49):19611–19616.
2. Metallo CM, Gameiro PA, Bell EL, et al. Reductive glutamine metabolism by IDH1 mediates lipogenesis under hypoxia. *Nature*. 2012;481(7381):380–384.
3. Semenza GL. HIF-1 mediates metabolic responses to intratumoral hypoxia and oncogenic mutations. *J Clin Invest*. 2013;123(9):3664–3671.
4. Forsythe JA, Jiang BH, Iyer NV, et al. Activation of vascular endothelial growth factor gene transcription by hypoxia-inducible factor 1. *Mol Cell Biol*. 1996;16(9):4604–4613.
5. Kim JW, Tchernyshyov I, Semenza GL, Dang CV. HIF-1-mediated expression of pyruvate dehydrogenase kinase: a metabolic switch required for cellular adaptation to hypoxia. *Cell Metab*. 2006;3(3):177–185.
6. Papandreou I, Cairns RA, Fontana L, Lim AL, Denko NC. HIF-1 mediates adaptation to hypoxia by actively downregulating mitochondrial oxygen consumption. *Cell Metab*. 2006;3(3):187–197.
7. Trayhurn P. Hypoxia and adipose tissue function and dysfunction in obesity. *Physiol Rev*. 2013;93(1):1–21.

8. **Pasarica M, Sereda OR, Redman LM, et al.** Reduced adipose tissue oxygenation in human obesity—evidence for rarefaction, macrophage chemotaxis and inflammation without an angiogenic response. *Diabetes*. 2008;58:718–725.
9. **Hosogai N, Fukuhara A, Oshima K, et al.** Adipose tissue hypoxia in obesity and its impact on adipocytokine dysregulation. *Diabetes*. 2007;56(4):901–911.
10. **Rausch ME, Weisberg S, Vardhana P, Tortoriello DV.** Obesity in C57BL/6J mice is characterized by adipose tissue hypoxia and cytotoxic T-cell infiltration. *Int J Obes (Lond)*. 2008;32:451–463.
11. **Ye J, Gao Z, Yin J, He Q.** Hypoxia is a potential risk factor for chronic inflammation and adiponectin reduction in adipose tissue of ob/ob and dietary obese mice. *Am J Physiol Endocrinol Metab*. 2007;293(4):E1118–E1128.
12. **He Q, Gao Z, Yin J, Zhang J, Yun Z, Ye J.** Regulation of HIF-1 α activity in adipose tissue by obesity-associated factors: adipogenesis, insulin, and hypoxia. *Am J Physiol Endocrinol Metab*. 2011;300(5):E877–E885.
13. **Wang B, Wood IS, Trayhurn P.** Dysregulation of the expression and secretion of inflammation-related adipokines by hypoxia in human adipocytes. *Pflugers Arch*. 2007;455(3):479–492.
14. **Trayhurn P, Wang B, Wood IS.** Hypoxia in adipose tissue: a basis for the dysregulation of tissue function in obesity? *Br J Nutr*. 2008;100(2):227–235.
15. **Fujisaka S, Usui I, Ikutani M, et al.** Adipose tissue hypoxia induces inflammatory M1 polarity of macrophages in an HIF-1 α -dependent and HIF-1 α -independent manner in obese mice. *Diabetologia*. 2013;56(6):1403–1412.
16. **Wood IS, de Heredia FP, Wang B, Trayhurn P.** Cellular hypoxia and adipose tissue dysfunction in obesity. *Proc Nutr Soc*. 2009;68(4):370–377.
17. **Halberg N, Khan T, Trujillo ME, et al.** Hypoxia-inducible factor 1 α induces fibrosis and insulin resistance in white adipose tissue. *Mol Cell Biol*. 2009;29(16):4467–4483.
18. **Sun K, Halberg N, Khan M, Magalang UJ, Scherer PE.** Selective inhibition of hypoxia-inducible factor 1 α ameliorates adipose tissue dysfunction. *Mol Cell Biol*. 2013;33(5):904–917.
19. **Jiang C, Qu A, Matsubara T, et al.** Disruption of hypoxia-inducible factor 1 in adipocytes improves insulin sensitivity and decreases adiposity in high-fat diet-fed mice. *Diabetes*. 2011;60(10):2484–2495.
20. **Krishnan J, Danzer C, Simka T, et al.** Dietary obesity-associated Hif1 α activation in adipocytes restricts fatty acid oxidation and energy expenditure via suppression of the Sirt2-NAD⁺ system. *Genes Dev*. 2012;26(3):259–270.
21. **Lee KY, Gesta S, Boucher J, Wang XL, Kahn CR.** The differential role of Hif1 β /Arnt and the hypoxic response in adipose function, fibrosis, and inflammation. *Cell Metab*. 2011;14(4):491–503.
22. **Lee YS, Kim JW, Osborne O, et al.** Increased adipocyte O₂ consumption triggers HIF-1 α , causing inflammation and insulin resistance in obesity. *Cell*. 2014;157(6):1339–1352.
23. **Regazzetti C, Peraldi P, Gremeaux T, et al.** Hypoxia decreases insulin signaling pathways in adipocytes. *Diabetes*. 2009;58(1):95–103.
24. **Yin J, Gao Z, He Q, Zhou D, Guo Z, Ye J.** Role of hypoxia in obesity-induced disorders of glucose and lipid metabolism in adipose tissue. *Am J Physiol Endocrinol Metab*. 2009;296(2):E333–E342.
25. **Kabayama K, Sato T, Saito K, et al.** Dissociation of the insulin receptor and caveolin-1 complex by ganglioside GM3 in the state of insulin resistance. The neck of caveolae is a distinct plasma membrane subdomain that concentrates insulin receptors in 3T3-L1 adipocytes. *Proc Natl Acad Sci USA*. 2007;104(34):13678–13683.
26. **Foti M, Porcheron G, Fournier M, Maeder C, Carpentier JL.** The neck of caveolae is a distinct plasma membrane subdomain that concentrates insulin receptors in 3T3-L1 adipocytes. *Proc Natl Acad Sci USA*. 2007;104(4):1242–1247.
27. **Stralfors P.** Caveolins and caveolae, roles in insulin signalling and diabetes. *Adv Exp Med Biol*. 2012;729:111–126.
28. **Hansen CG, Nichols BJ.** Exploring the caves: cavins, caveolins and caveolae. *Trends Cell Biol*. 2010;20(4):177–186.
29. **Bastiani M, Parton RG.** Caveolae at a glance. *J Cell Sci*. 2010;123(Pt 22):3831–3836.
30. **Parton RG, del Pozo MA.** Caveolae as plasma membrane sensors, protectors and organizers. *Nat Rev Mol Cell Biol*. 2013;14(2):98–112.
31. **Briand N, Dugail I, Le Lay S.** Cavin proteins: new players in the caveolae field. *Biochimie*. 2011;93(1):71–77.
32. **Razani B, Combs TP, Wang XB, et al.** Caveolin-1-deficient mice are lean, resistant to diet-induced obesity, and show hypertriglyceridemia with adipocyte abnormalities. *J Biol Chem*. 2002;277(10):8635–8647.
33. **Drab M, Verkade P, Elger M, et al.** Loss of caveolae, vascular dysfunction, and pulmonary defects in caveolin-1 gene-disrupted mice. *Science*. 2001;293(5539):2449–2452.
34. **Chadda R, Mayor S.** PTRF triggers a cave in. *Cell*. 2008;132(1):23–24.
35. **Hayer A, Stoeber M, Bissig C, Helenius A.** Biogenesis of caveolae: stepwise assembly of large caveolin and cavin complexes. *Traffic*. 2010;11(3):361–382.
36. **Hansen CG, Bright NA, Howard G, Nichols BJ.** SDPR induces membrane curvature and functions in the formation of caveolae. *Nat Cell Biol*. 2009;11(7):807–814.
37. **Hill MM, Bastiani M, Luetterforst R, et al.** PTRF-cavin, a conserved cytoplasmic protein required for caveola formation and function. *Cell*. 2008;132(1):113–124.
38. **McMahon KA, Zajicek H, Li WP, et al.** SRBC/cavin-3 is a caveolin adapter protein that regulates caveolae function. *EMBO J*. 2009;28(8):1001–1015.
39. **Liu L, Brown D, McKee M, et al.** Deletion of cavin/PTRF causes global loss of caveolae, dyslipidemia, and glucose intolerance. *Cell Metab*. 2008;8(4):310–317.
40. **Breen MR, Camps M, Carvalho-Simoes F, Zorzano A, Pilch PF.** Cholesterol depletion in adipocytes causes caveolae collapse concomitant with proteosomal degradation of cavin-2 in a switch-like fashion. *Plos One*. 2012;7(4):e34516.
41. **Kim CA, Delepine M, Boutet E, et al.** Association of a homozygous nonsense caveolin-1 mutation with Berardinelli-Seip congenital lipodystrophy. *J Clin Endocrinol Metab*. 2008;93(4):1129–1134.
42. **Hayashi YK, Matsuda C, Ogawa M, et al.** Human PTRF mutations cause secondary deficiency of caveolins resulting in muscular dystrophy with generalized lipodystrophy. *J Clin Invest*. 2009;119(9):2623–2633.
43. **Ding SY, Lee MJ, Summer R, Liu L, Fried SK, Pilch PF.** Pleiotropic effects of cavin-1 deficiency on lipid metabolism. *J Biol Chem*. 2014;289(12):8473–8483.
44. **Gustavsson J, Parpal S, Karlsson M, et al.** Localization of the insulin receptor in caveolae of adipocyte plasma membrane. *FASEB J*. 1999;13(14):1961–1971.
45. **Kimura A, Mora S, Shigematsu S, Pessin JE, Saltiel AR.** The insulin receptor catalyzes the tyrosine phosphorylation of caveolin-1. *J Biol Chem*. 2002;277(33):30153–30158.
46. **Cohen AW, Razani B, Wang XB, et al.** Caveolin-1-deficient mice show insulin resistance and defective insulin receptor protein expression in adipose tissue. *Am J Physiol Cell Physiol*. 2003;285(1):C222–C235.
47. **Plaisant M, Fontaine C, Cousin W, Rochet N, Dani C, Peraldi P.** Activation of hedgehog signaling inhibits osteoblast differentiation of human mesenchymal stem cells. *Stem Cells*. 2009;27(3):703–713.
48. **Rodriguez AM, Elabd C, Delteil F, et al.** Adipocyte differentiation of multipotent cells established from human adipose tissue. *Biochem Biophys Res Commun*. 2004;315(2):255–263.
49. **Cormont M, Tanti JF, Zahraoui A, Van Obberghen E, Tavitian A, Le Marchand-Brustel Y.** Insulin and okadaic acid induce Rab4 re-

- distribution in adipocytes. *J Biol Chem.* 1993;268(26):19491–19497.
50. Kilroy G, Burk DH, Floyd ZE. High efficiency lipid-based siRNA transfection of adipocytes in suspension. *PLoS One.* 2009;4(9):e6940.
 51. Bertola A, Bonnafous S, Anty R, et al. Hepatic expression patterns of inflammatory and immune response genes associated with obesity and NASH in morbidly obese patients. *Plos One.* 2010;5(10):e13577.
 52. Anty R, Bekri S, Luciani N, et al. The inflammatory C-reactive protein is increased in both liver and adipose tissue in severely obese patients independently from metabolic syndrome, type 2 diabetes, and NASH. *Am J Gastroenterol.* 2006;101(8):1824–1833.
 53. Anty R, Iannelli A, Patouraux S, et al. A new composite model including metabolic syndrome, alanine aminotransferase and cyto-keratin-18 for the diagnosis of non-alcoholic steatohepatitis in morbidly obese patients. *Aliment Pharmacol Ther.* 2010;32(11–12):1315–1322.
 54. Wallace TM, Levy JC, Matthews DR. Use and abuse of HOMA modeling. *Diabetes Care.* 2004;27(6):1487–1495.
 55. Bickel PE, Scherer PE, Schnitzer JE, OH P, Lisanti MP, Lodish HF. Flotillin and epidermal surface antigen define a new family of caveolae-associated integral membrane proteins. *J Biol Chem.* 1997;272(21):13793–13802.
 56. Rajendran L, Le Lay S, Illges H. Raft association and lipid droplet targeting of flotillins are independent of caveolin. *Biol Chem.* 2007;388(3):307–314.
 57. Rajendran L, Masilamani M, Solomon S, et al. Asymmetric localization of flotillins/reggies in preassembled platforms confers inherent polarity to hematopoietic cells. *Proc Natl Acad Sci USA.* 2003;100(14):8241–8246.
 58. Bastiani M, Liu L, Hill MM, et al. MURC/cavin-4 and cavin family members form tissue-specific caveolar complexes. *J Cell Biol.* 2009;185(7):1259–1273.
 59. Shoshani T, Faerman A, Mett I, et al. Identification of a novel hypoxia-inducible factor 1-responsive gene, RTP801, involved in apoptosis. *Mol Cell Biol.* 2002;22(7):2283–2293.
 60. Ellisen LW, Ramsayer KD, Johannessen CM, et al. REDD1, a developmentally regulated transcriptional target of p63 and p53, links p63 to regulation of reactive oxygen species. *Mol Cell.* 2002;10(5):995–1005.
 61. Regazzetti C, Bost F, Le Marchand-Brustel Y, Tanti JF, Giorgetti-Peraldi S. Insulin induces REDD1 expression through hypoxia-inducible factor 1 activation in adipocytes. *J Biol Chem.* 2010;285(8):5157–5164.
 62. Ye J. Emerging role of adipose tissue hypoxia in obesity and insulin resistance. *Int J Obes (Lond).* 2009;33(1):54–66.
 63. Parpal S, Karlsson M, Thorn H, Stralfors P. Cholesterol depletion disrupts caveolae and insulin receptor signaling for metabolic control via insulin receptor substrate-1, but not for mitogen-activated protein kinase control. *J Biol Chem.* 2001;276(13):9670–9678.
 64. Briand N, Prado C, Mabilieu G, et al. Caveolin-1 expression and cavin stability regulate caveolae dynamics in adipocyte lipid store fluctuation. *Diabetes.* 2014;63(12):4032–4044.
 65. Hansen CG, Shvets E, Howard G, Riento K, Nichols BJ. Deletion of cavin genes reveals tissue-specific mechanisms for morphogenesis of endothelial caveolae. *Nat Commun.* 2013;4:1831.
 66. Moren B, Shah C, Howes MT, et al. EHD2 regulates caveolar dynamics via ATP-driven targeting and oligomerization. *Mol Biol Cell.* 2012;23(7):1316–1329.
 67. Geiger K, Leiberer A, Muendlein A, et al. Identification of hypoxia-induced genes in human SGBS adipocytes by microarray analysis. *Plos One.* 2011;6(10):e26465.
 68. Leiberer A, Geiger K, Muendlein A, Drexel H. Hypoxia induces a HIF-1 α dependent signaling cascade to make a complex metabolic switch in SGBS-adipocytes. *Mol Cell Endocrinol.* 2014;383(1–2):21–31.
 69. Linden MA, Pincu Y, Martin SA, Woods JA, Baynard T. Moderate exercise training provides modest protection against adipose tissue inflammatory gene expression in response to high-fat feeding. *Physiol Rep.* 2014;2(7).
 70. Canello R, Henegar C, Viguerie N, et al. Reduction of macrophage infiltration and chemoattractant gene expression changes in white adipose tissue of morbidly obese subjects after surgery-induced weight loss. *Diabetes.* 2005;54(8):2277–2286.
 71. Rajab A, Straub V, McCann LJ, et al. Fatal cardiac arrhythmia and long-QT syndrome in a new form of congenital generalized lipodystrophy with muscle rippling (CGL4) due to PTRF-CAVIN mutations. *PLoS Genet.* 2010;6(3):e1000874.
 72. Cao H, Alston L, Ruschman J, Hegele RA. Heterozygous CAV1 frameshift mutations (MIM 601047) in patients with atypical partial lipodystrophy and hypertriglyceridemia. *Lipids Health Dis.* 2008;7:3.
 73. Gupta R, Toufaily C, Annabi B. Caveolin and cavin family members: dual roles in cancer. *Biochimie.* 2014;107PB:188–202.
 74. Shastry S, Delgado MR, Dirik E, Turkmen M, Agarwal AK, Garg A. Congenital generalized lipodystrophy, type 4 (CGL4) associated with myopathy due to novel PTRF mutations. *Am J Med Genet A.* 2010;152A(9):2245–2253.
 75. Nassoy P, Lamaze C. Stressing caveolae new role in cell mechanics. *Trends Cell Biol.* 2012;22(7):381–389.
 76. Bai L, Deng X, Li Q, et al. Down-regulation of the cavin family proteins in breast cancer. *J Cell Biochem.* 2012;113(1):322–328.